vienna2006

P056

Extended Elastic Impedance and Its Relation to AVO Crossplotting and Vp/Vs

G.J. Hicks* (Earthworks Environment & Resources) & A.M. Francis (Earthworks Environment & Resources)

SUMMARY

Extended Elastic Impedance (EEI) has proved to be a highly convenient framework for seismic AVO studies. EEI logs can be directly related to the petrophysical properties of interest and seismic EEI reflectivity volumes can be obtained directly from the prestack data via linear projection in sin2theta. The directness of the EEI method is one of its strengths, making it unnecessary to perform intermediate steps such as examining conventional AVO attributes (e.g., intercepts and gradients). Consequently it can be difficult for those more familiar with the conventional AVO analysis to understand the parallels between the two methods. Once these parallels are understood we show how they can be exploited to provide new AVO attributes for background Vs/Vp ratio and AVO class based on the EEI seismic projection method.

Summary

Extended Elastic Impedance (EEI) has proved to be a highly convenient framework for seismic AVO studies. EEI logs can be directly related to the petrophysical properties of interest and seismic EEI reflectivity volumes can be obtained directly from the prestack data via linear projection in $\sin^2\theta$. The directness of the EEI method is one of its strengths, making it unnecessary to perform intermediate steps such as examining conventional AVO attributes (e.g., intercepts and gradients). Consequently it can be difficult for those more familiar with the conventional AVO analysis to understand the parallels between the two methods. Once these parallels are understood we show how they can be exploited to provide new AVO attributes for background Vs/Vp ratio and AVO class based on the EEI seismic projection method.

Introduction

Conventional elastic impedance (EI) is defined as a function of the reflection angle, θ. Although EI based on the conventional 2-term AVO equation is only valid as a model to predict recorded prestack seismic data over the 0-30° angle range, it is defined mathematically over a 0-90° angle range which corresponds to a $\sin^2\theta$ range of 0-1. Whitcombe et al. (2002) recognized that outside of the 0-30° angle range, although EI is not valid for predicting prestack seismic data it may correspond with rock physics or petrophysical properties of interest. Whitcombe et al. (2002) therefore extended conventional EI so that it is defined for all values of $\sin^2\theta$ between positive and negative infinity. This is achieved by replacing $\sin^2\theta$ with a new function $\tan\chi$, such that $\sin^2\theta = \tan\chi$. This results in bounds on the angle χ of -90 to +90 degrees. The seismic data corresponding to EEI at a given χ angle can be constructed by performing a sample-by-sample linear projection of the recorded prestack amplitudes in $\sin^2\theta$.

The EEI log at $\chi = 0°$ is identical to the EI log at $\theta = 0°$, which is simply acoustic impedance. Whitcombe et al. (2002) demonstrates that EEI logs at certain other χ angles correspond to other important rock physics parameters, such as bulk modulus ($\chi = 12°$), shear modulus ($\chi = -51°$) and Lamé's constant ($\chi = 20°$) (assuming a constant relationship between sonic velocity and density expressed as a constant Gardner's parameter).

Although it can be interesting to estimate (relative changes in) rock-physics parameters directly from prestack seismic using the EEI method, rock-physics parameters are often secondary to predictions of reservoir properties. Estimates of porosity, fluid content and lithology are far more readably interpretable. Whitcombe et al. (2002) and Neves et al. (2004) show how different petrophysics logs can be predicted using the EEI method. Whitcombe et al. (2002) show that water saturation and gamma ray values can be predicted using the EEI method applied to data from the Forties field in the central North Sea, while Neves et al. (2004) show gamma ray prediction for a gas play in central Saudi Arabia. Both sets of authors calculate the correlation coefficients between each petrophysics log of interest and all the EEI logs between -90° and +90°. The strength of the correlations indicate how well a given petrophysics log can be predicted, which EEI log should be used, and how independently the petrophysics logs can be estimated.

Traditionally quantitative use of AVO information has usually involved IP-IS inversion followed by mapping the inverted IP-IS values to the most likely petrophysics parameter value using relations determined by IP-IS crossplotting. The strength of the EEI method is that it enables one to invert directly for an EEI volume that corresponds to a petrophysics parameter of interest. Although the directness of the method makes it highly efficient, the relationship between traditional AVO methods and EEI is not readily apparent. We hope that by clarifying the relation between AVO and EEI, the EEI method will become more transparent to those more familiar with conventional AVO analysis.

Extended Elastic Impedance and the AVO Crossplot

Whitcombe et al. (2002) give the scaled reflectivity related to an EEI log at a given χ as

$$R_S(\chi) = A\cos\chi + B\sin\chi \qquad (1)$$

where A and B are the AVO intercept and gradient from the commonly used 2-term Zoeppritz linearization, $R(\theta) = A + B\sin^2\theta$. Setting $R_S = 0$ gives the following relation

$$\tan\chi_0 = -A/B \qquad (2)$$

where χ_0 is the χ angle at which the reflectivity, as defined by the conventional 2-term AVO equation, is zero. We refer to this χ angle as the "minimum energy χ".

The angle in an AVO (A vs. B) crossplot from the negative B axis is defined by $\tan\phi = -A/B$. It is therefore apparent that $\chi_0 = \phi$; the EEI angle χ_0 is equal to the angle from the negative B axis in an AVO crossplot. Using this insight it is straightforward to interpret patterns seen in an AVO crossplot in terms of the equivalent EEI responses. Figure 1 shows a schematic AVO crossplot in which the zones corresponding to the different AVO classes are shown along a background shale trend. Points which plot along the shale trend have a constant AVO crossplot angle, ϕ, and hence are associated with a constant χ_0 angle. An EEI seismic projection at an angle of χ_0 is equivalent to calculating the distance in the crossplot from the shale trend line. Such a projection will be insensitive to shale-shale interfaces.

Figure 2 shows a similar AVO crossplot. The AVO responses at shale-brine sand interfaces for class I, II and III sands are shown by the blue squares (after Hilterman, 2001). The AVO responses for corresponding shale-gas sand interfaces are shown by green circles. Black arrows indicate the tie-lines between the brine and gas cases. Fluid substitution from brine to gas would cause the AVO response to change in the direction indicated by these arrows. An EEI seismic projection at a χ angle perpendicular to this direction yields the EEI seismic projection most sensitive to fluid changes. As indicated by Figure 2, this χ angle is typically a small positive value somewhat less than χ_0.

Examining correlation curves in order to select the χ angle at which the EEI logs best correspond to the petrophysical logs of interest, as done by Whitcombe et al. (2002) and Neves et al. (2004), is therefore equivalent to examining AVO crossplots based on elastic impedances calculated at the wells in order to determine if trends in the AVO crossplot correspond to the petrophysical parameters of interest.

Extended Elastic Impedance and AVO Class

Using equation (2) it is straightforward to relate the minimum energy χ angle to the AVO class of a given event. Castagna and Swan (1997) demonstrated how distinct sections of the AVO crossplot are associated with the different AVO classes. Young and LoPiccolo (2003) expanded the traditional AVO class classification to cover the entire AVO crossplot with 10 AVO types, the boundaries between which are lines which intercept the origin of the crossplot. In their classification Young and LoPiccolo (2003) rescale A and B so that they have the same dynamic range before crossplotting. This can be achieved by scaling A by a factor γ, where typically $\gamma \approx 4$. This yields the following equation for the angle ϕ' in the scaled AVO crossplot:

$$\tan\phi' = -\gamma A / B = \gamma\tan\chi_0 . \qquad (3)$$

The resulting angle ϕ' can be used to calculate the standard AVO class, as shown in Figure 1, or to calculate the more comprehensive AVO type.

Extended Elastic Impedance and Background Vs/Vp

The relationship between the AVO crossplot and the background Vs/Vp ratio was first demonstrated by Castagna and Swan (1997) and Castagna et al (1998) who show that, assuming a Gardner relation between acoustic velocity and density, lines of constant background Vs/Vp pass through the origin of the AVO crossplot. The background Vs/Vp is therefore related to the angle from the negative B axis, ϕ, with increasing ϕ (in the anticlockwise direction) corresponding to decreasing Vs/Vp (Figure 3). However it should be noted that estimating the background Vs/Vp from ϕ is only valid where the background response is observed (strictly where only small changes in velocity are observed); this method is therefore not valid where localized amplitude anomalies are present.

Since we have shown in this abstract that ϕ is related to the EEI method it is straightforward to also relate the EEI method directly to the background Vs/Vp ratio. Rearranging equation (12) from Castagna et al. (1998) one obtains

$$\left(\frac{\beta}{\alpha}\right)^2 = \frac{1}{9}\left(1 - \frac{5}{4}\frac{B}{A}\right). \qquad (4)$$

Substituting in $\tan\chi_0 = -A/B$ we obtain the following relation between Vs/Vp and the minimum energy χ angle:

$$\left(\frac{\beta}{\alpha}\right)^2 = \frac{1}{9}\left(1 + \frac{5}{4\tan\chi_0}\right). \qquad (5)$$

Equation (5) can be used to estimate the background Vs/Vp ratio from the EEI seismic projection angle which results in the minimum energy seismic projection.

Application

The equations given above can be used to estimate the AVO class of seismic events and the background Vs/Vp ratio based on the minimum energy χ angle associated with EEI projection. Although well logs are usually required in order to calibrate EEI seismic projections to the petrophysical properties of interest (as described in the introduction), well data are not required to calculate the background Vs/Vp and AVO class attributes described above. This makes them particularly useful in exploration areas.

Figure 4 shows EEI logs calculated as a function of χ for all angles between -90 and +90 degrees (Francis and Hicks, 2006). The minimum energy χ angle (χ_0) is indicated by the dashed line. The slow variation of χ_0 with depth indicates a changing Vs/Vp ratio, while local changes indicate changes in AVO class associated with particular events.

References

Castagna, J. P., and Swan, H. W., 1997, Principles of AVO crossplotting: THE LEADING EDGE, **16,** no. 04, 337-342.

Castagna, J. P., Swan, H. W. and Foster, D. J., 1998, Framework for AVO gradient and intercept interpretation: GEOPHYSICS, Soc. of Expl. Geophys., **63,** 948-956.

Francis, A., and Hicks, G. J., 2006, Porosity and shale volume estimation for the Ardmore Field using extended elastic impedance, 68th Mtg.: Eur. Assn. Geosci. Eng. (Submitted).

Hilterman, F. J., 2001, Seismic amplitude interpretation: 2001 Distinguished Instructor Short Course, Distinguished Instructor Series, No. 4, Soc. of Expl. Geophys., 235.

Neves, F.A., Mustafa, H. M. and Rutty, P.M., 2004, Interpreter's Corner—Pseudo-gamma ray volume from extended elastic impedance inversion for gas exploration: THE LEADING EDGE, **23,** no. 06, 536-540.

Whitcombe, D. N., Connolly, P. A., Reagan, R. L. and Redshaw, T. C., 2002, Extended elastic impedance for fluid and lithology prediction: GEOPHYSICS, Soc. of Expl. Geophys., **67,** 63-67.

Young, R. A., and LoPiccolo, R. D., 2003, A comprehensive AVO classification: THE LEADING EDGE, **22,** no. 10, 1030-1037.

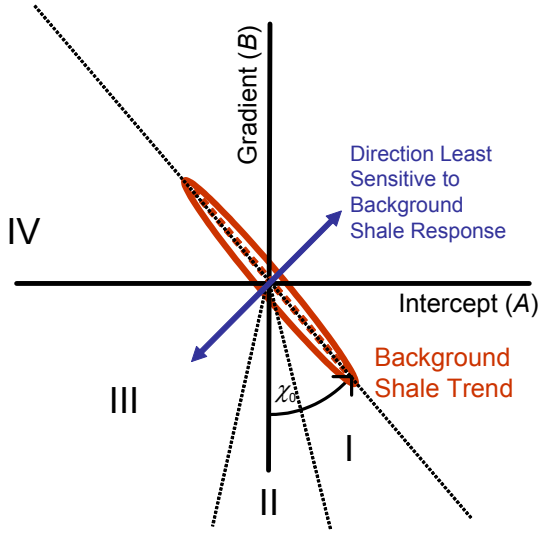

Figure 1: Schematic AVO crossplot showing regions corresponding to Class I-IV reflections. The background shale trend plots at an angle of χ_0 from the negative *B* axis.

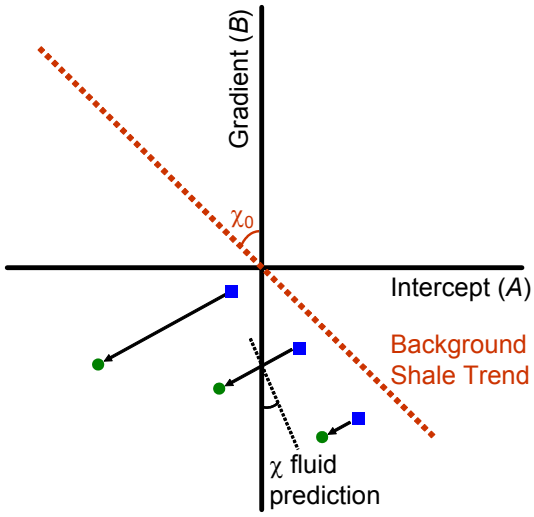

Figure 2: Schematic AVO crossplot showing shale-brine sand (blue squares) and shale-gas sand (green circles) responses.

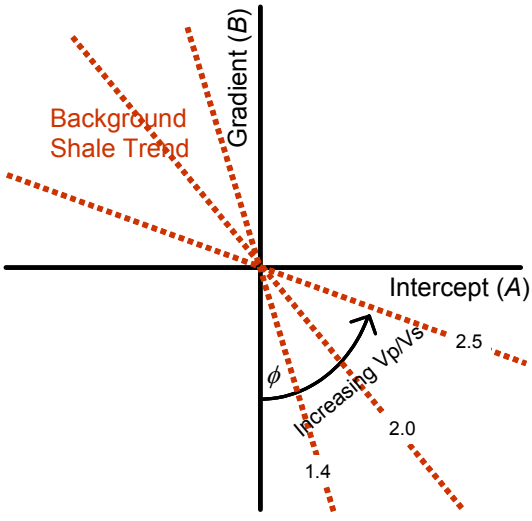

Figure 3: Schematic AVO crossplot showing how increasing Vp/Vs is related to the angle the background shale trend makes with the negative *B* axis. After Castagna and Swan (1997).

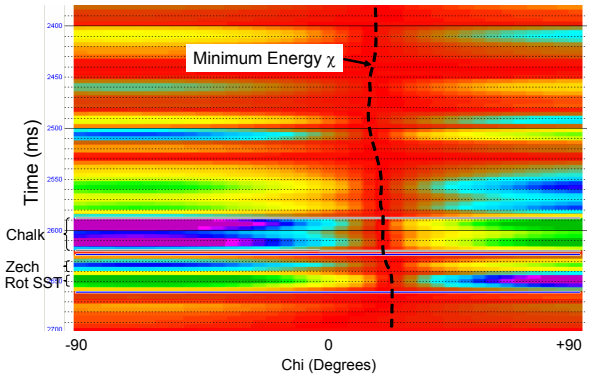

Figure 4: EEI logs as a function of χ. Changes in the minimum energy χ angle with depth are indicated by the dashed line.